

# Packet-Level Traffic Modeling with Heavy-Tailed Payload and Inter-Arrival Distributions for Digital Twins

Enes Koktas and Peter Rost

**Abstract**—Digital twins of radio access networks require packet-level traffic generators that reproduce the size and timing of packets while remaining compact and easy to recalibrate as traffic changes. We address this need with a hybrid generator that combines a small hidden Markov model, which captures buffering, streaming, and idle states, with a mixture density network that models the joint distribution of payload length and inter arrival time (IAT) in each state using Student-t mixtures. The state space and emission family are designed to handle heavy-tailed IATs by anchoring an explicit idle state in the tail and allowing each component to adapt its tail thickness. We evaluate the model on public traces of web, smart home, and encrypted media traffic and compare it with recent neural network and transformer based generators as well as hidden Markov baselines. Across most datasets and metrics, including average per-flow cumulative distribution functions, autocorrelation based measures of temporal structure, and Wasserstein distances between flow descriptors, the proposed generator matches the real traffic most closely in the majority of cases while using orders of magnitude fewer parameters. The full model occupies around 0.2 MB in our experiments, which makes it suitable for deployment inside digital twins where memory footprint and low-overhead adaptation are critical.

**Index Terms**—Heavy tail, Hidden Markov model, Mixture density network, Mobile communication, Network digital twin, Synthetic traffic generation

## I. INTRODUCTION

IN recent years, digital twins (DTs) have received more attention because they enable optimization, autonomy, predictive maintenance, real-time monitoring, root cause analysis, problem detection, and risk-free what-if scenario analysis for present and future communication protocols and operations. A DT framework consists of three main components: the real space, the virtual space, and a link that allows communication between the two [1]. The virtual space replicates the physical counterpart in real-time. DTs may play a major part in next generation networks. Existing network operations are often already automated but always need feedback from an operating network. Various use cases of DTs at different stages of a communication system require different resolution of available statistics. Exemplary use cases include handover optimization, resource allocation, network planning, and traffic offloading. A network DT can combine data collection and processing, and AI modeling to examine the network’s current condition,

This research was supported by the German Federal Ministry of Research, Technology and Space (BMFTR) under grant number 16KIS2259 (SUSTAINET-inNOvAte).

forecast future patterns, and facilitate predictive maintenance [2].

### A. Problem definition

A network DT that represents a radio access network (RAN) should reproduce how traffic is offered to the network at packet level, not only at a coarse rate or volume level, because schedulers, link adaptation, buffer management, and congestion control all depend on the timing and size of packets. Real packet traces are often heavy tailed, meaning they are characterized by rare but extremely large values, where the measurements on wired and wireless links show heavy-tailed OFF periods and session durations [3]. In our datasets a small fraction of packets are separated by gaps that are orders of magnitude longer than the median, which influences whether buffers drain, inactivity timers expire, and flows return from idle. If a generator underestimates the frequency or length of such gaps, the DT may underestimate delay, queue occupancy, and timeout probability, and thus provide overly optimistic performance predictions. At the same time, streaming full packet traces from the physical network to the virtual space and retraining a large model whenever conditions change is usually not practical due to data security risks, limited backhaul, and additional overhead. The problem we address in this work is therefore to design a compact and interpretable packet generator that can be trained on an initial dataset, that captures the heavy-tailed structure of payload size and IATs so that the DT can follow traffic changes without requiring continuous transfer of raw traces.

### B. Related Work

Early synthetic traffic generators such as TRex, NS-3, and Harpoon combine packet or flow replay with simulation models that are configured by hand [4]. They are practical for reproducing known scenarios but rely on user defined templates that must be tuned by experts for each test case. As a result they struggle to match the detailed behavior of packet sizes and IATs observed in modern traces. Recent work has therefore turned to data driven generative models that learn directly from packet traces. Several articles apply generative adversarial networks (GANs) to synthesize network flows, with recurrent layers in the generator and discriminator to better capture temporal patterns [5], [6]. Hybrid schemes combine autoencoders with Wasserstein GANs to operate in a latent space, for example by encoding Internet of Things

packet size sequences, sampling new latent codes with a GAN, and decoding them into synthetic flows [7]. NeCSTGen takes a similar latent approach: a variational autoencoder compresses packets, a Gaussian mixture and recurrent neural network model the cluster transitions, and the resulting chain is used to produce packet, flow, and aggregate level traces [8]. These neural generators can reproduce a broad class of marginal statistics, but adversarial training is sensitive to initialization and loss design. More recently, transformer based sequence models have been proposed for network traffic analysis and generation. A pre-trained transformer is proposed in [9] with a linear attention mechanism that extends the usable context to up to 12 032 tokens per flow and achieves state of the art performance on long flow classification tasks while producing synthetic flows that closely resemble real traffic. Such architectures are attractive when large unlabeled collections of data and central compute resources are available. In a packet level DT where many individual RAN scenarios must be adapted on site, however, the size of these models, their memory footprint at long context length, and the need to fine tune or condition them for each environment makes it difficult to deploy them on edge hardware. In [10], the authors fit two independent hidden Markov models (HMMs), one for payload length and one for IAT, to video streaming and gaming traces using the Baum–Welch algorithm. This captures the one dimensional marginals of size and timing but might miss their joint dependence, which is important for buffer dynamics and delay.

### C. Contribution

In this article we propose a compact packet level traffic generator for network DTs that factorizes each flow into a small hidden state process and a mixture density network (MDN). The HMM captures coarse states such as buffering, steady streaming, and idle, while the MDN learns the joint distribution of payload length and IAT within each state. The design is explicitly tailored to heavy tailed IATs: we augment the state space with an idle state that is anchored in the tail of the timing distribution and replace Gaussian components by Student-t kernels so that rare long gaps and bursts receive appropriate probability mass.

## II. DATASET AND NOTATION

We evaluate the proposed generator on four packet level traces that cover web browsing, smart home traffic, and encrypted media streaming. The first two traces contain hypertext transfer protocol (HTTP) and datagram protocol (UDP) traffic from [8]. The other two traces contain Facebook audio and Facebook video sessions from the virtual private network traffic dataset described in [11]. In all four datasets we keep the original flow identifiers and retain only the fields needed by our model, namely payload length and IAT for each packet. Table I summarizes the main characteristics of these traces in terms of number of flows, total packets, packet count per flow, volume, and average flow duration. The HTTP and UDP traces are small but contain many short flows, while the Facebook

TABLE I: Summary statistics of the datasets.

Feature Name	HTTP	UDP	Facebook Audio	Facebook Video
File Size (MB)	0.31	0.30	2.4	4.4
Total Flows	718	588	250	173
Total Packets	10,000	10,000	91,737	156,982
Average Pkts./Flow	13.9	17.0	366.9	907.4
Total Volume (MB)	3.86	3.91	10.57	162.67
Average Flow Duration (s)	2.95	8.87	97.36	55.78

audio and Facebook video traces have fewer flows with longer sessions and heavier tails.

We work at packet level and represent each captured flow as an ordered sequence of packet tuples. The raw dataset consists of one row per packet in the form *flow index, payload length, time difference*, where flow index is an identifier that groups packets into flows, payload length is the application payload in bytes, and time difference is the IAT between consecutive packets in seconds.

Let  $\mathbb{R}_+ = \{x \in \mathbb{R} \mid x > 0\}$  denote the set of positive real numbers. For a given flow index  $i$  with length  $L_i \in \mathbb{N}$ , the  $t$ -th packet is denoted by the vector  $\mathbf{x}_{i,t} \in \mathbb{R}_+^2$  with

$$\mathbf{x}_{i,t} = [p_{i,t}, \delta_{i,t}]^\top, \quad (1)$$

where  $p_{i,t}$  is the payload length in bytes and  $\delta_{i,t}$  is the IAT in seconds, defined as the time interval between the arrival of the current packet  $t$  and the previous packet  $t - 1$ .

To make the statistics well-conditioned while preserving the heavy right tail of IATs that motivated our model design, we cap only unrealistically large gaps during preprocessing used to fit scalers (e.g., one hour for IATs), and bound payloads to the valid Ethernet maximum transmission unit (MTU) range seen in the traces.

For learning, we apply a monotone normalizing transform componentwise,

$$u_{i,t}^{(1)} = \ln(p_{i,t}), \quad (2)$$

$$u_{i,t}^{(2)} = \ln(\delta_{i,t}), \quad (3)$$

where  $\ln(\cdot)$  denotes the natural logarithm, and then normalize with moments estimated on training flows only. The normalized packet is

$$\mathbf{z}_{i,t} = \left( [u_{i,t}^{(1)}, u_{i,t}^{(2)}]^\top - \mathbf{m} \right) \oslash \mathbf{r}, \quad (4)$$

where  $\mathbf{m} \in \mathbb{R}^2$  and  $\mathbf{r} \in \mathbb{R}_+^2$  are the mean and standard deviation of (2) and (3) computed over all packets in the training flows, and  $\oslash$  denotes componentwise division. We split the dataset into training and testing sets by flow to preserve the flow structure. During synthesis, each test flow keeps its original identifier and length, which enables paired, flow-wise evaluations between real and synthetic sequences.

The dataset exhibits heavy-tailed IAT. We quantify this tail by computing a tail threshold  $\tau_\delta \in \mathbb{R}_+$  defined as the empirical 99.8th percentile of (3) over all packets in the training set. This scalar is used to define a tail-aware “idle” state in the state space when required, without discarding the extremes.

Let  $\ell_i = \ln(L_i)$  be the log transformed flow length, and let  $m_\ell$  and  $s_\ell$  be its training mean and standard deviation; we define the scalar

$$\xi_i = \frac{\ell_i - m_\ell}{s_\ell}, \quad (5)$$

which remains constant across packets of flow  $i$ . For state-related notation, we use  $K \in \mathbb{N}$  for the number of latent states and  $k \in \{1, \dots, K\}$  for the index of a latent state. The latent state at packet  $(i, t)$  is  $s_{i,t} \in \{1, \dots, K\}$ , and

$$\mathbf{e}^{(k)} \in \{0, 1\}^K \quad (6)$$

denotes the one-hot vector of state  $k$ . We follow this section's notations in the remainder of the manuscript when specifying the hidden-state process, tail-aware state augmentation, and the MDN.

### III. SYSTEM MODEL

Packet traffic can be viewed as flows that move across a small set of latent states such as buffering, steady streaming, and idle. A compact HMM can determine when the flow enters a state, how long it stays, and when it leaves. The HMM can summarize the burstiness and dwell times that appear in real traces, capturing packet level temporal structure of a flow. A flexible MDN then specifies the distribution of packet attributes within the chosen state. It shapes payload length and IAT jointly and preserves their dependence. By separating state switching from per-packet variability, the model decouples the temporal evolution from the geometry of packets. This design makes the generator interpretable and flexible to retrain within a DT loop. The model remains sensitive to rare but important events such as long idle gaps and heavy-tailed bursts. The result is a compact system, shown in Fig. 1, which captures the states that drive traffic while retaining enough expressiveness to reproduce extremes and cross-dependencies observed in practice.

Hidden Markov models provide a compact way to describe time series that move between a small number of latent states [12]. They assume an unobserved state that evolves as a Markov chain over time and, at each step, produces an observation from a state specific distribution. In our setting the states represent regimes such as buffering, steady streaming, and idle, and the observations are the normalized payload length and IAT of each packet. Standard HMM training uses the expectation-maximization (EM) algorithm, which alternates between an expectation step (E-step) that computes state posteriors given the current parameters and a maximization step (M-step) that updates the parameters to increase the data likelihood [12]. Such training often starts from random parameters or from a simple clustering of the data. On heavy-tailed packet traces this initialization can lead to unstable state distributions and poor local optima. We therefore devote the next subsection to a tailored initialization that already encodes an explicit idle state in the tail, initializes the core states from data driven clusters, and adds weak priors on the transition probabilities. This makes the HMM more stable from the first EM iterations and yields state sequences that can reliably supervise the MDN.

#### A. Hidden Markov model: Initialization

We first fit a compact HMM with single-component diagonal Gaussian emissions to obtain per-packet state assignments along each flow. The goal of this stage is not to be the final

generator but to discover coherent states and provide reliable posteriors for the supervised training of the MDN. The HMM parameters are collected in

$$\Theta = \{\boldsymbol{\alpha}, \mathbf{A}, \{\boldsymbol{\mu}_k, \boldsymbol{\Sigma}_k\}_{k=1..K}\}, \quad (7)$$

where  $\boldsymbol{\alpha} \in [0, 1]^K$  is the initial-state distribution whose entries add up to one, and  $\mathbf{A} \in [0, 1]^{K \times K}$  is the transition matrix whose rows add up to one,  $\boldsymbol{\mu}$  are the per-state means, and

$$\boldsymbol{\Sigma} = \{\boldsymbol{\Sigma}_k \in \mathbb{R}_+^2\} \quad (8)$$

collects the per-state variance vectors. The diagonal covariance used in the Gaussian kernels is  $\text{diag}(\boldsymbol{\Sigma}_k)$ .

Heavy right tails in IAT demand an explicit idle state rather than forcing a single Gaussian to stretch over orders of magnitude. We therefore start from a core number of states  $K_{\text{core}} \in \mathbb{N}$  and create an idle state  $K = K_{\text{core}} + 1$  when the training traffic exhibits a meaningful tail. We normalize  $\tau_\delta$  through

$$v_\delta = \frac{\tau_\delta - m^{(2)}}{r^{(2)}}, \quad (9)$$

where  $m^{(2)}$  and  $r^{(2)}$  are the second entries of  $\mathbf{m}$  and  $\mathbf{r}$  defined in (4). If the fraction of packets above  $v_\delta$  on training flows exceeds a small threshold  $\theta_{\text{tail}} \in (0, 1)$ , we activate the idle. Otherwise, we keep  $K = K_{\text{core}}$ . This rule activates the extra state precisely when the trace contains sufficiently many long gaps to justify a dedicated state, which stabilizes posteriors and reduces the tendency of EM to inflate variances in all states to cover extremes.

We initialize the core Gaussian emissions from the joint geometry of payload and timing. Following the HMM practice, where state-dependent Gaussians are initialized from a clustering step before EM [12], we run  $k$ -means on the normalized training packets. Specifically, we apply  $k$ -means with  $K_{\text{core}}$  clusters to the pooled set of normalized packets in  $\mathbf{z}$ -space obtained by concatenating all training flows. Let  $\{\mathbf{c}_k\}_{k=1}^{K_{\text{core}}} \subset \mathbb{R}^2$  denote the resulting centroids, and let  $\mathbf{v}_k \in \mathbb{R}_+^2$  denote the componentwise empirical variance of the packets assigned to centroid  $\mathbf{c}_k$ . We then initialize core state  $k$  with mean and diagonal covariance  $\boldsymbol{\mu}_k = \mathbf{c}_k$ , and

$$\boldsymbol{\Sigma}_k = \mathbf{v}_k + \varepsilon_0 \mathbf{1}, \quad (10)$$

where  $\mathbf{1}$  is the length-two vector of ones and  $\varepsilon_0 > 0$  is a small variance floor that prevents degenerate covariances.

When the idle state is active we place its initial mean at a stable, interpretable location. Denote by  $\rho_z \in \mathbb{R}$  the median of the first coordinate of all training packets in  $\mathbf{z}$ -space. The idle mean is then

$$\boldsymbol{\mu}_K = \begin{bmatrix} \rho_z \\ v_\delta \end{bmatrix}, \quad \boldsymbol{\Sigma}_K = \begin{bmatrix} \chi \\ 1 \end{bmatrix} \quad (11)$$

with a broad variance level  $\chi > 0$  that allows the EM step to adapt to the precise spread of long gaps. Initializing the timing coordinate exactly at  $v_\delta$  has two effects. First, it creates a clear basin that attracts packets near and above the tail onset, which improves the separation between core and idle states. Second, it prevents the core states from inflating their variances to accommodate rare long pauses, which would blur

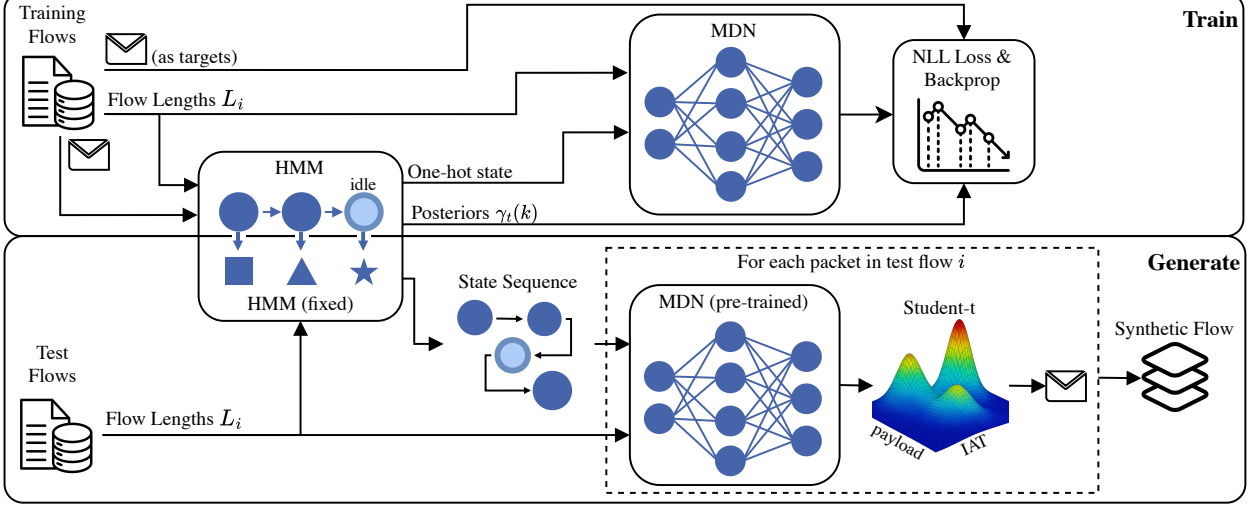


Fig. 1: Training and generation pipeline of the proposed traffic generator.

state boundaries and degrade the quality of the posteriors. Unlike the generic  $k$ -means initializing above, anchoring a dedicated idle state at a fixed  $v_\delta$  is specific to heavy-tailed packet IAT and, to our knowledge, is not part of standard HMM initializations [12].

The start distribution is initialized as  $\alpha_k = 1/K$ . To stabilize early EM iterations we add weak Dirichlet pseudo-counts to the rows of the transition matrix  $\mathbf{A}$ , which encourages state continuity but becomes negligible as more data are observed. For the idle state, we use a stronger self pseudo-count and very small pseudo-counts toward core states so that long gaps are captured while transitions back to core states remain possible. The exact prior and its effect on dwell times are discussed in Section III–III-B.

After each M-step we enforce a minimal variance level, renormalize transition rows, and reset any non-finite parameters. In a standard HMM, the latent states are not observed, so the training procedure needs the probability of each state at each time index given the whole sequence. The forward-backward algorithm provides exactly these per-time state probabilities by combining information from the past and the future of the same sequence [12]. We apply this inference separately on each flow using its own length  $L_i$ , which avoids learning artificial transitions across flows and yields reliable dwell times. These precautions keep the HMM stable and guarantee that the state posteriors are well behaved across packet scales.

Each element of the initialization is tied to a failure mode we observed in real packet traces. The idle state isolates the rare but operationally important long gaps so that core states specialize in active behavior. Initializing with  $k$ -means in the joint space of payload and timing encourages cross-feature coherence and reduces sensitivity to random initializations. Dirichlet priors on transitions encode only weak persistence assumptions. They improve dwell-time realism early in training and are essential when traces are short or dominated by a few bursts. Finally, the variance floor and post-EM sanity

checks harden the procedure against numerical collapse in heavy tails. Together these choices yield clean state posteriors and a transparent transition structure that the MDN can reliably refine in the next stage.

We note that we do not discover the true semantic states or their cardinality from data. The model uses a small state budget  $K_{\text{core}}$  that is a tunable hyperparameter, typically ranging from 2 to 4. It is set by the practitioner or selected with a light model-selection rule on training flows. The goal is a compact HMM that yields stable posteriors and a controllable generator rather than an unsupervised extraction of behavioral modes. This choice reflects the DT setting, where reproducibility and low overhead retuning are preferable to open-ended state discovery.

### B. Hidden Markov model: State process and inference

The HMM is a  $K$ -state first order Markov chain that evolves along each flow and selects a state for every packet. We denote the latent state sequence by  $s_{i,1:L_i}$  with  $s_{i,t} \in \{1, \dots, K\}$ . The chain is parameterized by  $\alpha$  and  $\mathbf{A}$  with non-negative rows that sum up to one. Conditioned on the state  $s_{i,t} = k$ , the normalized packet  $\mathbf{z}_{i,t}$  is drawn from a diagonal Gaussian with mean  $\mu_k$  and variance vector  $\Sigma_k$ . The joint model for one flow is

$$p(s_{i,1:L_i}, \mathbf{z}_{i,1:L_i}) = \alpha_{s_{i,1}} \prod_{t=2}^{L_i} A_{s_{i,t-1}, s_{i,t}} \times \prod_{t=1}^{L_i} \mathcal{N}(\mathbf{z}_{i,t}; \mu_{s_{i,t}}, \text{diag}(\Sigma_{s_{i,t}})) \quad (12)$$

At this stage we restrict the covariances to diagonal form so that the HMM remains compact, numerically stable under EM updates, and fast to re-estimate. Cross-feature dependence between payload and IAT is mainly handled by the MDN later. This division of roles keeps the HMM focused on dwell times and state switching without having to stretch Gaussian clouds across heavy right tails.

*Inference and learning.* We estimate  $\Theta$  in (7) on multiple independent flows by concatenating per-flow sequences and supplying a lengths vector  $L_i$  so that forward-backward is reset at each flow boundary. It allows the algorithm to sum the expected counts (the estimated number of times states and transitions occurred) across all flows, effectively performing a joint update as per the multi-sequence Baum-Welch algorithm in [12], implemented via [13]. This enables HMM to estimate the parameters by EM over training flows while respecting the flow boundaries. The E-step uses the standard forward-backward recursions on each flow  $i$  to compute the state posteriors

$$\gamma_{i,t}^{(k)} = p(s_{i,t} = k \mid \mathbf{z}_{i,1:L_i}), \quad (13)$$

where  $\gamma_{i,t}^{(k)} \in [0, 1]$  is the posterior probability that packet  $(i, t)$  belongs to state  $k$ , satisfying

$$\sum_{k=1}^K \gamma_{i,t}^{(k)} = 1, \quad (14)$$

and the two-slice marginals

$$\zeta_{i,t}^{(k,\ell)} = p(s_{i,t} = k, s_{i,t+1} = \ell \mid \mathbf{z}_{i,1:L_i}). \quad (15)$$

The state posteriors act as weights for the emission update in the M-step. The M-step starts with the covariance, which we update from weighted second central moments:

$$\Sigma_k = \frac{S_k}{R_k} + \varepsilon_0 \mathbf{1}, \quad (16)$$

where  $\varepsilon_0 > 0$  keeps variances positive in heavy-tail segments. The effective sample size (responsibility mass) using (13) is

$$R_k = \sum_i \sum_{t=1}^{L_i} \gamma_{i,t}^{(k)}, \quad (17)$$

the weighted sum of squared deviations is

$$S_k = \sum_i \sum_{t=1}^{L_i} \gamma_{i,t}^{(k)} (\mathbf{z}_{i,t} - \boldsymbol{\mu}_k) \odot (\mathbf{z}_{i,t} - \boldsymbol{\mu}_k), \quad (18)$$

where  $\odot$  denotes elementwise product. The state mean uses the same weights as (17),

$$\boldsymbol{\mu}_k = \frac{\sum_i \sum_{t=1}^{L_i} \gamma_{i,t}^{(k)} \mathbf{z}_{i,t}}{R_k}. \quad (19)$$

We update the state process from expected start and transition counts, which are accumulated across flows as

$$N_k^{\text{start}} = \sum_i \gamma_{i,1}^{(k)}, \quad (20)$$

and

$$N_{k,\ell} = \sum_i \sum_{t=1}^{L_i-1} \zeta_{i,t}^{(k,\ell)}, \quad (21)$$

using (15). The normalized updates are

$$\alpha_k = \frac{N_k^{\text{start}}}{\sum_{m=1}^K N_m^{\text{start}}}, \quad (22)$$

$$A_{k,\ell} = \frac{N_{k\ell} + \Lambda_{k,\ell}}{\sum_{m=1}^K (N_{km} + \Lambda_{km})}. \quad (23)$$

Here  $\Lambda \in \mathbb{R}_+^{K \times K}$  is a Dirichlet prior with

$$\Lambda_{ij} = \begin{cases} \lambda_{\text{self}}, & i = j, i \neq K, \\ \lambda_{\text{off}}, & i \neq j, i \neq K, \\ \lambda_{\text{idle}}, & i = j = K, \\ \lambda_{\text{leak}}, & i = K, j \neq K, \end{cases} \quad (24)$$

where  $\Lambda$  collects Dirichlet pseudo-counts on transitions, and  $\lambda_{\text{self}}, \lambda_{\text{off}}, \lambda_{\text{idle}}, \lambda_{\text{leak}} \in \mathbb{R}_+$  are scalar hyperparameters. The  $K$ -th row corresponds to the idle state when present. By construction the update in (23) is row-normalized, so rows of  $\mathbf{A}$  sum up to one. Flow boundaries are enforced in (21) by omitting  $t = L_i$ . We iterate E- and M-steps with these definitions until the relative improvement in average log-likelihood stalls or a fixed iteration cap is reached. After each M-step we apply the variance floor in (16), replacing any non-finite entries in (19) by neutral values to maintain numerical stability, and renormalize rows of  $\mathbf{A}$ . The resulting  $\Theta$  parameterize the next E-step and later drive state path sampling during synthesis.

*Start, transitions, and dwell realism.* The initial distribution is set to  $\alpha_k = 1/K$  at the beginning of training and then updated during the training process described. This choice reflects the fact that application flows can begin in any state. The transition prior  $\Lambda$  retains the diagonal preference from initialization. Core rows use a moderate self-transition pseudo-count  $\lambda_{\text{self}}$  and a smaller off-diagonal level  $\lambda_{\text{off}}$ , which reduces early oscillations without biasing the learned chain once sufficient data accumulate. For the idle state, its row receives a stronger self-prior  $\lambda_{\text{idle}}$  and a very small leak level  $\lambda_{\text{leak}}$ . This mirrors the behavior that once a flow enters a long waiting period it tends to stay there for many packets. In a finite-state HMM, the expected dwell time in state  $i$  is

$$E[D_i] = 1 / (1 - a_{ii}), \quad (25)$$

so increasing the idle state's  $a_{ii}$  encodes longer idle spans in the simplest possible way [12]. This design is consistent with Internet traffic measurements, where OFF periods are empirically long and often heavy-tailed, which is a key mechanism behind self-similar burstiness at the aggregate level [3]. At the individual user level inactive and active periods exhibit no characteristic length, allowing arbitrarily long idle or busy spans with non-negligible probability [14]. We use the same prior across datasets. It acts only as a weak stabilizer during early EM iterations and is quickly dominated by the data. As a result of these initialization modifications, the final transition matrix  $\mathbf{A}$  produces realistic dwell times while remaining data-driven.

We use the soft posteriors  $\gamma_{i,t}^{(k)}$  rather than a hard Viterbi path to supervise the MDN later. This keeps information about uncertainty in parts of a flow where states switch, for example near the start or end of buffering periods. With soft labels the network can use packets that belong partly to two states instead of treating them as mislabelled. During synthesis we do not replay a single best state sequence from training. We generate new state paths by sampling from the learned  $\alpha$  and  $\mathbf{A}$ . This reintroduces randomness into the state process and produces

synthetic flows whose variability is closer to what we see in the test flows.

In summary, we keep the HMM compact so that it remains stable and easy to retrain in a digital-twin loop. Diagonal Gaussian emissions with a variance floor and a Dirichlet prior on transitions prevent numerical problems on heavy-tailed IATs and short traces. This layer is only used to produce well-behaved state posteriors along each flow, which then supervise the MDN in the next subsection.

### C. Mixture density network

The MDN refines each latent state with a conditional mixture that is expressive enough to reproduce the joint geometry of packet payload and IAT and stable enough to train with a small number of hyperparameters. The network conditions on the state of the packet and the length of the flow that the packet is supposed to be located in. Conditioning on the state allows the network to learn the shape of the mixture densities that best represent the typical payload and IAT values that are most likely to be observed within that particular state. The choice of including flow length as a conditioning feature comes from our observations in [15, Fig. 4]. We observed that the model struggles to capture IAT characteristics of the flows consisting of only one to five packets in the UDP dataset. The flow-length (packet-count) feature enables the model to differentiate packet characteristics between long and short flows.

We concatenate the state code with the normalized flow length and write the input feature at packet  $(i, t)$  under state  $k$  using (5) and (6) as

$$\mathbf{h}_{i,t}^{(k)} = [\mathbf{e}^{(k)}, \xi_i]^\top \in \mathbb{R}^{K+1}. \quad (26)$$

The network maps  $\mathbf{h}_{i,t}^{(k)}$  to the parameters of a mixture with  $M$  components that models the normalized target  $\mathbf{z}_{i,t}$ . In the prior version we used Gaussian kernels for these components, which worked well on light and medium tails but consistently under-estimated the probability of extreme IATs in applications such as Facebook video calls [15]. To handle these heavy right tails without changing the overall architecture, we replace each Gaussian component by a Student- $t$  kernel and let the network learn a degrees-of-freedom parameter per component [16].

The MDN outputs the parameters of the conditional Student- $t$  mixture in (32). We use  $M \in \mathbb{N}$  for the number of mixture components and  $m \in \{1, \dots, M\}$  for the component index. Given the conditioning vector  $\mathbf{h}$ , it produces mixture weights  $\omega(\mathbf{h}) \in \mathbb{R}_+^M$  with

$$\sum_{m=1}^M \omega_m(\mathbf{h}) = 1, \quad (27)$$

together with a component mean  $\kappa_m(\mathbf{h}) \in \mathbb{R}^2$ , a positive component scale  $\sigma_m(\mathbf{h}) \in \mathbb{R}_+^2$  that acts as a per-coordinate standard deviation, and degrees of freedom  $\nu_m(\mathbf{h}) \in \mathbb{R}_{>1}$ . Smaller  $\nu_m(\mathbf{h})$  yields heavier tails and assigns non-negligible mass to long IATs and occasional payload bursts, whereas larger values approach Gaussian-like behavior. Each mixture component is a diagonal bivariate Student- $t$  in the normalized

packet space. The diagonal form keeps the parameter count small and numerically stable, while the mixture captures cross-coordinate dependence without introducing full covariances. In the implementation,  $\omega(\mathbf{h})$  is obtained with a softmax layer to satisfy (27),  $\sigma_m(\mathbf{h})$  use a softplus activation with a small floor, and  $\nu_m(\mathbf{h})$  use a softplus followed by a constant floor that enforces  $\nu_m(\mathbf{h}) > 1$ . The MDN is a feed-forward network with two tanh-activated hidden layers of width  $H$ , and we keep the same compact configuration across datasets with  $M = 32$  components,  $H = 128$  hidden units, and one learned  $\nu_m$  per component.

Training follows maximum likelihood with soft supervision from the bootstrap HMM. The general formula for the univariate Student- $t$  density with location  $\kappa \in \mathbb{R}$ , positive scale  $\sigma \in \mathbb{R}_+$ , and degrees of freedom  $\nu \in \mathbb{R}_{>1}$  can be written as in [16, Eq. (3)]:

$$t_\nu(y | \kappa, \sigma) = c(\nu, \sigma) \left( 1 + \frac{1}{\nu} \left( \frac{y - \kappa}{\sigma} \right)^2 \right)^{-\frac{\nu+1}{2}}, \quad (28)$$

where the normalizing constant is

$$c(\nu, \sigma) = \frac{\Gamma((\nu+1)/2)}{\Gamma(\nu/2)\sqrt{\nu\pi}\sigma}, \quad (29)$$

where  $\Gamma(\cdot)$  is the gamma function. Taking natural logarithm gives

$$\begin{aligned} \ln t_\nu(y | \kappa, \sigma) &= \log c(\nu, \sigma) - \frac{\nu+1}{2} \\ &\quad \times \log \left( 1 + \frac{1}{\nu} \left( \frac{y - \kappa}{\sigma} \right)^2 \right). \end{aligned} \quad (30)$$

For component  $m$  and coordinate  $d \in \{1, 2\}$  the network outputs  $\kappa_m^{(d)}(\mathbf{h})$ ,  $\sigma_m^{(d)}(\mathbf{h})$ , and  $\nu_m(\mathbf{h})$ . The corresponding diagonal bivariate Student- $t$  density is the product of its univariate factors,

$$t_m(\mathbf{z} | \mathbf{h}) = \prod_{d=1}^2 t_{\nu_m(\mathbf{h})} \left( z^{(d)} | \kappa_m^{(d)}(\mathbf{h}), \sigma_m^{(d)}(\mathbf{h}) \right), \quad (31)$$

where the same  $\nu_m(\mathbf{h})$  is shared across coordinates and each coordinate has its own scale. The conditional mixture density used by the MDN is

$$p_\varphi(\mathbf{z} | \mathbf{h}) = \sum_{m=1}^M \omega_m(\mathbf{h}) t_m(\mathbf{z} | \mathbf{h}), \quad (32)$$

where  $\varphi$  collects all MDN weights and biases. The per-sample Student- $t$  negative log-likelihood is

$$\ell_t(\mathbf{z}_{i,t}; \mathbf{h}_{i,t}^{(k)}, \varphi) = -\log p_\varphi(\mathbf{z}_{i,t} | \mathbf{h}_{i,t}^{(k)}). \quad (33)$$

Expanding (32) with (31) and (28) shows that  $\ell_t$  is the negative log of a mixture of diagonal bivariate Student- $t$  components, with the constant and  $\log(1 + (\cdot)^2/\nu_m)$  terms coming from (30) and accumulated across  $d$  and  $m$ .

The MDN is trained on mini-batches  $\mathcal{B}$  drawn from the training packets. For each  $(i, t) \in \mathcal{B}$  we plug the observed  $\mathbf{z}_{i,t}$  into (33) and minimize the weighted objective

$$\mathcal{L}(\varphi) = \sum_{(i,t) \in \mathcal{B}} w_{i,t} \ell_t(\mathbf{z}_{i,t}; \mathbf{h}_{i,t}^{(k)}, \varphi), \quad (34)$$

where  $w_{i,t}$  are packet weights defined by the HMM posteriors and balanced across states in the next paragraph. This process is equivalent to standard maximum-likelihood training of a conditional density model. The network sees packets from the dataset together with their state and flow length features, and adjusts  $\varphi$  so that the density defined in (32) assigns high probability to the training packets. Sampling from the mixture in (32) happens only in the synthesis stage described later.

The MDN dataset is formed by concatenating per-state slices. For each state  $k$  we keep packet  $(i, t)$  if the posterior  $\gamma_{i,t}^{(k)}$  from the bootstrap HMM exceeds a small threshold. The idle state uses a lower threshold so that rare long idle packets are not discarded. For every retained packet we create a target  $\mathbf{z}_{i,t}$ , an input  $\mathbf{h}_{i,t}^{(k)}$ , and a weight  $w_{i,t} = \gamma_{i,t}^{(k)}$ . Inside each state these posteriors act as soft labels, so packets with higher state probability have proportionally more influence on the loss. To prevent very frequent states from dominating the objective, we multiply all weights of a given state by a constant so that the total weight per state stays on a comparable scale.

During synthesis, the HMM provides a state sequence for each test flow. For packet  $t$  in state  $k$ , the MDN evaluates  $\omega, \varphi$  at  $\mathbf{h}_{i,t}^{(k)}$ , draws a component index from  $\omega$  and samples a diagonal bivariate Student- $t$ . The result is mapped back to the original domain by inverting the normalization and the log transforms and clip payload and IAT to the observed operational ranges (MTU and a practical timeout). An optional temperature on the component sampling for the idle state makes extremely long gaps marginally more likely.

In summary, the Student- $t$  mixture lets the MDN capture rare but important extremes without making sampling complicated. Using diagonal components in a mixture gives a stable way to model joint shapes with a moderate number of parameters. The state encoding tells the network which traffic state it is in, and the flow-length input passes session-scale effects down to individual packets. We train the MDN with weights derived from the HMM posteriors so that it learns from the state structure without being dominated by a single state. Together, these choices make the MDN both robust in practice and easy to interpret.

#### IV. RESULTS

The evaluation focuses on the three aspects that matter for a packet level DT: how well the marginal distributions are matched, how realistic the temporal dynamics are, and how much diversity the generator produces compared to the real traces. Here, diversity refers to coverage at the dataset level, meaning that the synthetic set should reproduce the range of flow characteristics observed in the real traces rather than concentrating on a small subset of typical flows. We therefore combine average per flow cumulative distribution functions (CDFs) of payload length and IAT, an autocorrelation (AC) based measure of temporal similarity, and a Wasserstein based measure of how well the distribution of flow descriptors is covered. We compare our model to state of the art traffic generators mentioned in Section I-I-B, which we implemented to the best of our knowledge. For a fair comparison, the models use the same pre- and post-processing steps and the same flow

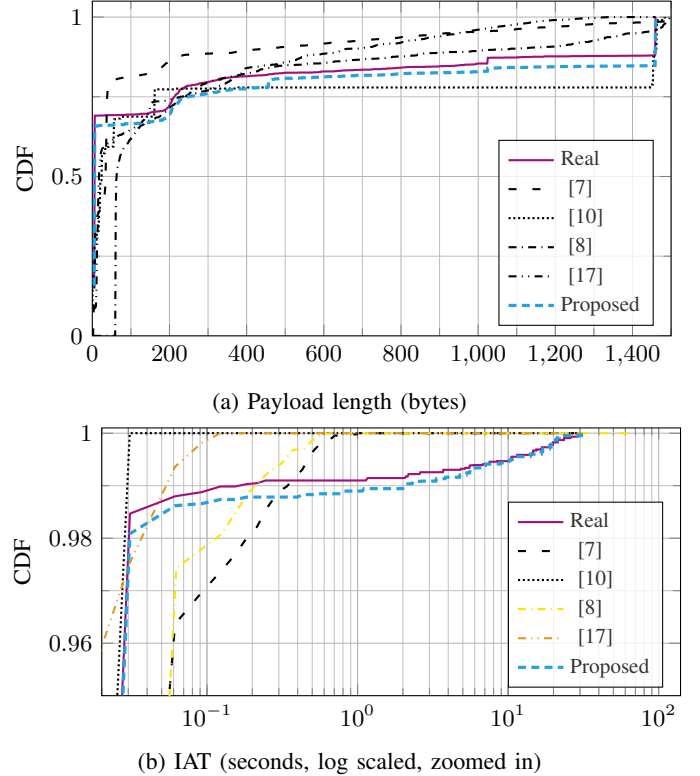
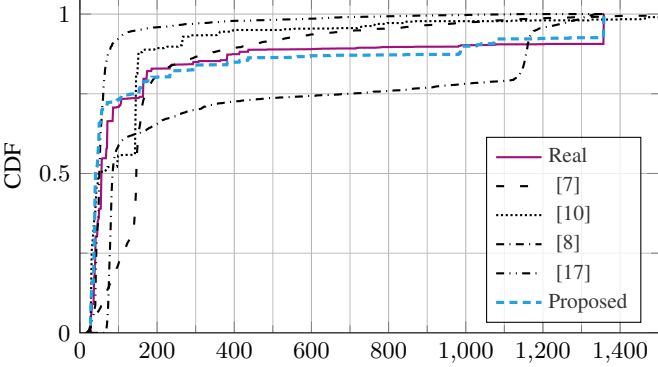


Fig. 2: Average per-flow CDF comparison of payload length and IAT for HTTP traffic.

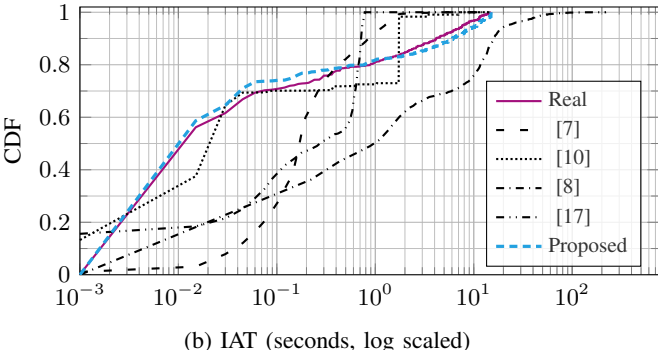
wise train/test split as our method. The models are evaluated on the same four datasets introduced in Section II.

Average per flow CDFs of various applications are shown in Figs. 2, 3, 4 and 5. The CDF plots show that the proposed hybrid generator tracks the real payload and IAT distributions closely for each scenario. For payloads, the synthetic CDFs almost overlay the real one across the full range from a few bytes up to large application data units, while the competing generators either collapse too much probability mass on a few sizes or fail to reproduce the fraction of maximum sized packets. For IATs the proposed model follows the real CDFs from the sub millisecond region up to long idle periods, whereas several baselines either produce overly regular streams or cut off the rare but important multi second gaps. The Facebook video trace in Fig. 5 is more challenging because payloads and timing are heavy tailed and flows contain a mix of interactive control and media segments, yet the proposed model again stays close to the real CDFs, with small discrepancies only at the very longest gaps.

AC has been used in traffic measurements to characterize dependence and burstiness over multiple time scales [18]. We measure temporal structure by computing, for each flow, the empirical AC functions of payload length and IAT, averaging these over flows, and then taking the root mean squared difference between the real and synthetic AC vectors at lags 1 through 20. Using per-flow AC avoids mixing traffic from different flows, and the choice of 20 lags reflects that in all datasets the AC of payload length and IAT decays close to zero within this range; including larger lags mainly averages



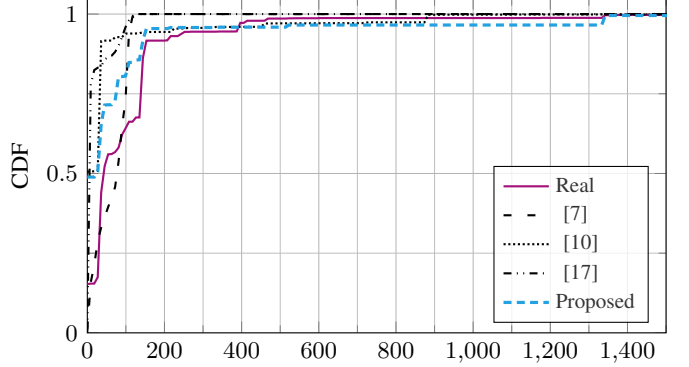
(a) Payload length (bytes)



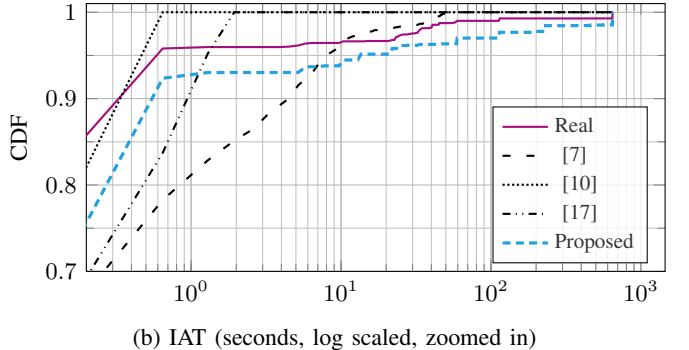
(b) IAT (seconds, log scaled)

Fig. 3: Average per-flow CDF comparison of payload length and IAT for UDP traffic.

over near-zero values and reduces the numerical scale of the metric without changing the relative ranking of the generators. To assess diversity we compare empirical distributions of flow level descriptors between real and synthetic traffic using a Wasserstein distance (WD). Wasserstein metrics are well suited for this purpose because they measure how much probability mass has to be transported to turn one distribution into another, which has made them a standard tool for comparing probability measures and evaluating generative models [19]. We compute WD at the level of the complete dataset rather than per flow, which reflects how well the generator covers the payload sizes and IATs observed in the dataset. We calculate both AC function based error and WD on log transformed synthetic and test data, which compresses the heavy right tails of payloads and IATs so that rare long gaps do not dominate the metrics while preserving the relative ranking between generators. The results are given in Table II, where boldface entries indicate the best result within each dataset and metric. The results show that the proposed generator keeps the Wasserstein distances smallest or close to the smallest across all datasets and achieves low AC based errors, especially for IAT, indicating that it reproduces both the heavy tailed and short range temporal structure of the traces better than the other generators. The absolute scale of the AC error is mainly set by the maximum lag, here lags one through twenty, and by the heaviness of the tails in each dataset, so the relative differences between models are the more informative indicator of how well they preserve the dependence between packet sizes and timing over consecutive arrivals.



(a) Payload length (bytes)



(b) IAT (seconds, log scaled, zoomed in)

Fig. 4: Average per-flow CDF comparison of payload length and IAT for Facebook audio traffic.

Among the baselines, the model in [9] is the closest competitor to our method in the CDFs plots. We therefore discuss it here in more detail. We implemented [9] using a compact decoder only transformer trained on quantized payload and IAT tokens. On the Facebook video trace, which is approximately 5 MB, the training plus generation takes about 1 min 20 s for the transformer, whereas our generator takes about 7 min, mainly due to the Student- $t$  negative log-likelihood in (33) that evaluates log and gamma functions. Further implementation optimization could reduce runtime, which we leave for future work. On Facebook video, the transformer recovers the bulk of the marginal payload and IAT distributions in Fig. 5. At temperature 1.0 (by default) it overemphasizes central values and under represents near second and multi second gaps. We added 1.5 temperature at generation, which smoothed the CDFs and brought the marginal fits close to those of the proposed model. This fidelity, however, comes at a substantially higher model size: the hybrid HMM of our approach uses approximately 0.0031 MB of parameters, the MDN emission adds about 0.161 MB, and the complete generator therefore occupies around 0.164 MB with roughly 42,000 trainable weights, whereas the TrafficGPT [9] variant in our experiments contains about 885,000 parameters and a footprint of 4.38 MB, more than twenty times as many weights and over twenty five times the memory requirement. In a centrally deployed setting with access to large collections of raw packet captures (about 190 gigabytes as in [9]) such a transformer is attractive, while our compact hybrid model is better suited to many small RAN

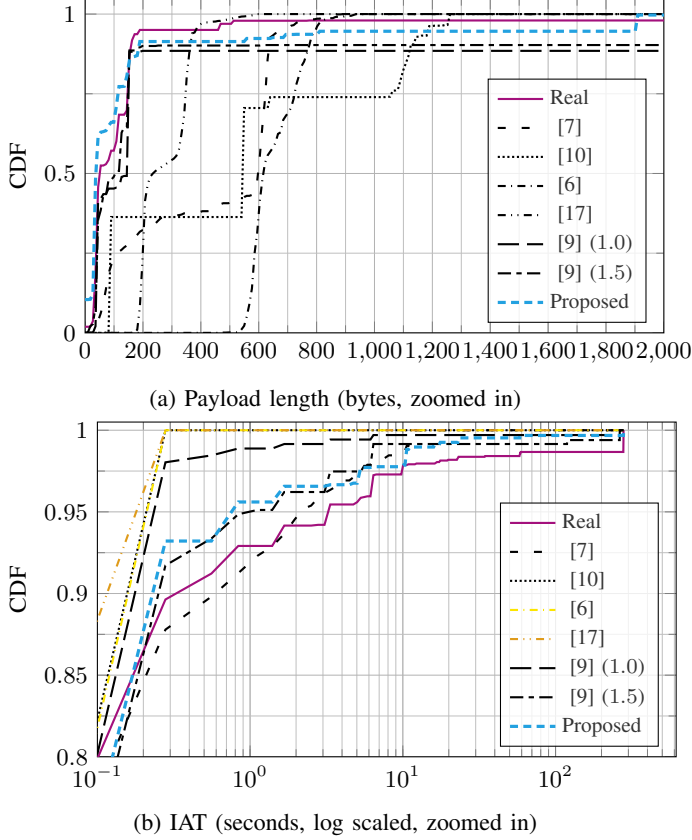


Fig. 5: Average per-flow CDF comparison of payload length and IAT for Facebook video traffic.

TABLE II: Comparison of temporal and diversity metrics of different models on various datasets.

Model	Dataset	AC		WD	
		Payload	IAT	Payload	IAT
Proposed	HTTP	0.09	<b>0.04</b>	<b>0.14</b>	<b>0.02</b>
	UDP	0.10	<b>0.07</b>	0.20	<b>0.06</b>
	Facebook Audio	<b>0.09</b>	<b>0.08</b>	0.62	0.44
	Facebook Video	<b>0.12</b>	<b>0.14</b>	<b>0.77</b>	0.47
[7]	HTTP	<b>0.04</b>	0.12	1.13	0.03
	UDP	0.16	0.28	0.90	0.22
	Facebook Audio	0.28	0.27	1.94	<b>0.29</b>
	Facebook Video	0.20	0.25	2.13	<b>0.34</b>
[10]	HTTP	0.13	0.06	0.75	<b>0.02</b>
	UDP	0.17	0.12	0.30	0.07
	Facebook Audio	0.15	0.12	<b>0.36</b>	0.48
	Facebook Video	0.13	<b>0.14</b>	2.85	0.50
[17]	HTTP	0.09	0.05	0.84	<b>0.02</b>
	UDP	0.10	0.11	0.75	0.16
	Facebook Audio	0.12	0.09	1.52	0.42
	Facebook Video	0.18	0.17	2.05	0.49
[9]	HTTP	<b>0.04</b>	0.42	0.50	0.06
	UDP	<b>0.08</b>	0.13	<b>0.16</b>	<b>0.06</b>
	Facebook Audio	0.10	0.15	1.27	0.51
	Facebook Video	0.14	0.16	0.94	0.39

DTs where low memory pressure and fast retraining under local traffic changes are more important than marginal gains on a single trace.

## V. CONCLUSION

In this article we presented a compact packet level traffic generator for network DTs that couples a small HMM with a Student t mixture density emission model to handle heavy tailed payloads and IATs. The tail anchored idle state and flow aware conditioning allow the model to reproduce buffering, streaming, and idle phases together with realistic joint distributions of packet sizes and gaps over several orders of magnitude. Across multiple datasets, it matches marginal distributions, temporal autocorrelation, and flow diversity more closely than recent neural, transformer, and HMM baselines in most cases, while keeping a memory footprint in the order of a few tenths of a MB. The separation between HMM and MDN makes the generator interpretable and easy to recalibrate from compact statistics when traffic evolves, which supports practical deployment inside resource constrained network DTs.

## REFERENCES

- [1] S. Mihai, M. Yaqoob, D. V. Hung, W. Davis, P. Towakel, M. Raza, M. Karamanoglu, B. Barn, D. Shetve, R. V. Prasad, H. Venkataraman, R. Trestian, and H. X. Nguyen, "Digital twins: A survey on enabling technologies, challenges, trends and future prospects," *IEEE Commun. Surveys Tuts.*, vol. 24, no. 4, pp. 2255–2291, 2022.
- [2] C. Zhou, H. Yang, X. Duan, D. Lopez, A. Pastor, Q. Wu, M. Boucadair, and C. Jacquet, "Network digital twin: Concepts and reference architecture," Internet Engineering Task Force, Tech. Rep., Mar. 2024, work in Progress. [Online]. Available: <https://datatracker.ietf.org/doc/draft-irtf-nmrg-network-digital-twin-arch/05/>
- [3] M. Crovella and A. Bestavros, "Self-similarity in world wide web traffic: evidence and possible causes," *IEEE/ACM Trans. Netw.*, vol. 5, no. 6, pp. 835–846, 1997.
- [4] A. Chu, X. Jiang, S. Liu, A. Bhagoji, F. Bronzino, P. Schmitt, and N. Feamster, "Feasibility of state space models for network traffic generation," in *Proc. of the 2024 SIGCOMM Workshop on Networks for AI Comput.*, ser. NAIC '24. New York, NY, USA: Association for Computing Machinery, 2024, p. 9–17. [Online]. Available: <https://doi.org/10.1145/3672198.3673792>
- [5] Z. Lin, A. Jain, C. Wang, G. Fanti, and V. Sekar, "Using GANs for sharing networked time series data: Challenges, initial promise, and open questions," in *Proc. of the ACM Internet Meas. Conf.*, ser. IMC '20. New York, NY, USA: Association for Computing Machinery, 2020, p. 464–483. [Online]. Available: <https://doi.org/10.1145/3419394.3423643>
- [6] T. Li, S. Hui, S. Zhang, H. Wang, Y. Zhang, P. Hui, D. Jin, and Y. Li, "Mobile user traffic generation via multi-scale hierarchical GAN," *ACM Trans. Knowl. Discov. Data*, vol. 18, no. 8, Jul. 2024. [Online]. Available: <https://doi.org/10.1145/3664655>
- [7] M. R. Shahid, G. Blanc, H. Jmila, Z. Zhang, and H. Debar, "Generative deep learning for internet of things network traffic generation," in *2020 IEEE 25th Pacific Rim Int. Symp. on Dependable Comput. (PRDC)*, 2020, pp. 70–79.
- [8] F. Meslet-Millet, S. Mouysset, and E. Chaput, "NeCSTGen: An approach for realistic network traffic generation using deep learning," in *IEEE Global Commun. Conf. (GLOBECOM)*, 2022, pp. 3108–3113.
- [9] J. Qu, X. Ma, and J. Li, "TrafficGPT: Breaking the token barrier for efficient long traffic analysis and generation," 2024. [Online]. Available: <https://arxiv.org/abs/2403.05822>
- [10] H. Redžović, A. Smiljanić, and M. Bjelica, "IP traffic generator based on hidden Markov models," in *Proc. of 4th Int. Conf. on Electr., Electron. and Comput. Eng. (IcETRAN)*, Jun 2017, pp. TEI2.3.1–6.
- [11] G. Draper-Gil, A. H. Lashkari, M. S. I. Mamun, and A. A. Ghorbani, "Characterization of encrypted and VPN traffic using time-related," in *Proc. of the 2nd Int. Conf. on Inf. Syst. Secur. and Privacy (ICISSP)*, 2016, pp. 407–414.
- [12] L. Rabiner, "A tutorial on hidden markov models and selected applications in speech recognition," *Proc. IEEE*, vol. 77, no. 2, pp. 257–286, 1989.
- [13] D. Cournapeau, F. Pedregosa, G. Varoquaux, S. Lebedev, A. Lee, and M. Danielson, "hmmlearn: Hidden markov models in python," 2015, accessed Nov. 12, 2025. [Online]. Available: <https://github.com/hmmlearn/hmmlearn>

- [14] W. Leland, M. Taqqu, W. Willinger, and D. Wilson, "On the self-similar nature of ethernet traffic (extended version)," *IEEE/ACM Trans. Netw.*, vol. 2, no. 1, pp. 1–15, 1994.
- [15] E. Koktas and P. Rost, "State aware traffic generation for real-time network digital twins," in *2025 IEEE 36th IEEE Int. Symp. Pers. Indoor Mob. Radio Commun. (PIMRC)*, 2025, pp. 1–6.
- [16] K. L. Lange, R. J. A. Little, and J. M. G. Taylor, "Robust statistical modeling using the t distribution," *J. Amer. Statist. Assoc.*, vol. 84, no. 408, pp. 881–896, 1989. [Online]. Available: <https://doi.org/10.1080/01621459.1989.10478852>
- [17] J. Yoon, D. Jarrett, and M. van der Schaar, "Time-series generative adversarial networks," in *Adv. in Neural Inf. Process. Syst.*, H. Wallach, H. Larochelle, A. Beygelzimer, F. d'Alché-Buc, E. Fox, and R. Garnett, Eds., vol. 32. Curran Associates, Inc., 2019. [Online]. Available: [https://proceedings.neurips.cc/paper\\_files/paper/2019/file/c9e5e5f26cd17ba6216bbe2a7d26d490-Paper.pdf](https://proceedings.neurips.cc/paper_files/paper/2019/file/c9e5e5f26cd17ba6216bbe2a7d26d490-Paper.pdf)
- [18] V. Paxson and S. Floyd, "Wide area traffic: the failure of poisson modeling," *IEEE/ACM Trans. on Netw.*, vol. 3, no. 3, pp. 226–244, 1995.
- [19] G. Peyré and M. Cuturi, "Computational optimal transport," 2020. [Online]. Available: <https://arxiv.org/abs/1803.00567>